RSC Advances

ROYAL SOCIETY OF CHEMISTRY

www.rsc.org/advances

Cite this: DOI: 10.1039/c0xx00000x

www.rsc.org/xxxxxx

ARTICLE TYPE

Cysteine-based fluorescence "turn-on" sensors for Cu^{2+} and Ag^{+}

V. Haridas,*[a] P. P. Praveen Kumar[a] and Cherumuttathu H. Suresh[b]

Received (in XXX, XXX) Xth XXXXXXXXX 20XX, Accepted Xth XXXXXXXXX 20XX
DOI: 10.1039/b000000x

We designed and synthesized two metal ion binding molecules 3a and 3b based on cysteine. In 3a, pyrene is used as a fluorescent probe, while 3b contains tryptophan, which acts as a fluorescent probe as well as facilitates metal ion binding. Detailed spectroscopic, calorimetric, microscopic and computational studies revealed the binding mode and the plausible structures of the complexes.

Selective detection of metal ions using fluorescence spectroscopy is a method of choice particularly owing to its high sensitivity and simplicity of measurement.[1] Detection by turn-on/off fluorescence will depend on the mode of interaction of the sensing molecule with the guest molecule.[2] Therefore, the design and synthesis of fluorescent organic molecules with appropriate coordination pocket for the desired specificity for the metal ion are challenging. Proteins are highly superior in terms of their specificity and metal ion binding ability.[3] The metal ion binding capacity of proteins is due to the specific amino acid side chains, for example, the well studied zinc finger proteins bind the zinc ion using the imidazole and the thiolate side chains of histidine and cysteine respectively.[4] In a similar way, the indole moiety of tryptophan (Trp) is involved in metal binding in CusF protiens.[5] However the ability of these amino acid side-chains are not completely exploited for the design of synthetic metal ion sensors.[6]

Here in this study, we use cysteine to design fluorescent sensors for metal ion binding. The C-terminus of the cysteine was conjugated to fluorophores such as pyrene or tryptophan to obtain compounds **3a** or **3b** respectively. Pyrene is an excellent fluorophore with a distinct monomer and excimer emission bands,[7] whereas tryptophan is a naturally occurring amino acid which shows fluorescence as well as the ability to bind metal ion through its indole side chain. Trp can provide the most potent cation-π binding sites.[8]

[a]*Department of Chemistry, Indian Institute of Technology Delhi, Hauz Khas-110016, New Delhi, India. Tel: (+91)11-26591380; E-mail: h.haridas@hotmail.com, haridasv@iitd.ac.in*
[b]*Computational Modeling and Simulation, National Institute for Interdisciplinary Science and Technology, (NIIST-CSIR) Thiruvananthapuram – 695019, India*

† Electronic Supplementary Information (ESI) available: Full experimental procedures, DFT studies, spectroscopic data, NMR (^{1}H and ^{13}C) and ITC titration data. See DOI: 10.1039/b000000x/

In order to synthesize **3a** and **3b**, the thiol group of L-cysteine was protected as S-*t*-butylcysteine, which was then coupled with pyrene methylamine/L-tryptophan methyl ester (TrpOMe) under dicyclohexycarbodiimide (DCC) and N-hydroxysuccinimide (NHS) coupling condition to afford **3a** and **3b** respectively.

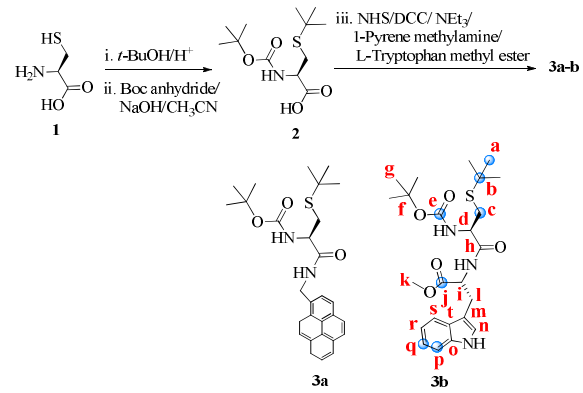

Scheme 1. Synthesis of **3a** and **3b**.

Compounds **3a** and **3b** were then investigated for their metal uptake potential. UV-visible spectroscopic studies revealed considerable changes in the spectra of **3a** and **3b** upon the addition of Cu^{2+} and Ag^{+} respectively (see ESI†, Fig. S1). Among the metal ions tested, addition of Cu^{2+} to **3a**, resulted in formation of a new peak at 298 and 403 nm with two isobestic points, indicating the complex formation between **3a** and Cu^{2+} (see ESI†, Fig. S1c). Studies on the complexing abilities of various metal cations (Na^{+}, K^{+}, Cs^{+}, Ag^{+}, Mg^{2+}, Ba^{2+}, Cd^{2+}, Zn^{2+}, Pb^{2+}, Mn^{2+}, Cu^{2+}, Hg^{2+}, Sn^{2+} and Fe^{3+}) towards **3a** demonstrated that it has higher selectivity for Cu^{2+} than other metal ions tested (see ESI†, Fig. S1a).

Excitation of **3a** at 340 nm resulted in two emission bands at 378 and 399 nm corresponding to the monomer emission bands of pyrene.[7] The addition of Cu^{2+} to **3a** resulted in the formation of new emission band at 470 nm corresponding to the excimer of pyrene with a concomitant decrease in the monomer emission bands. The excimer band intensity increased upon the addition of Cu^{2+} indicating that binding of Cu^{2+} brings two pyrene moieties in close proximity. The observed fluorescence "turn-on" upon metal ion binding is a remarkable property of **3a**, since heavy metals generally causes a quenching effect on the fluorescence (see ESI†, Figs. 1a and S2a).[9] The complex formation between **3a** and Cu^{2+} was further confirmed by mass spectrometric analysis,

which showed a peak at 1066.3750 corresponding to [2 . **3a** + Cu^{2+} + Na^{+}] (see ESI†, Fig. S3). Job's plot further proved the formation of the 2:1 complex between **3a** and Cu^{2+} (see ESI†, Fig. S4). The excitation spectra of **3a** + Cu^{2+} showed a red shift of 7 nm indicating a static type excimer (see ESI†, Fig. S5).[7b] The fluorescence decay monitored at 390 nm and 470 nm indicated no change in the decay time of the free and complexed species, characteristic of static excimer formation (see ESI†, Fig. S6 and Table S1).[10] Competitive binding studies of **3a** with various metal ions (see ESI†, Fig. S7) showed that **3a** can detect Cu^{2+} in the presence of other metal ions with a detection limit of 4 μM and a binding constant of $1.24x10^{5}$ M^{-2}.[11]

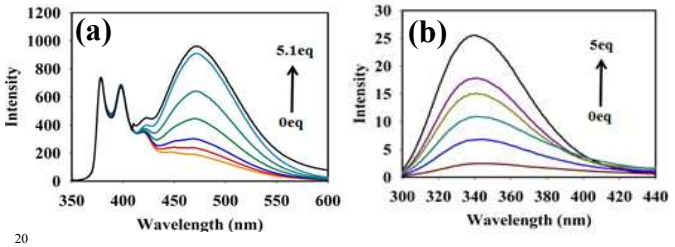

Fig 1. (a) Fluorescence spectra of **3a** ($1.2x10^{-5}$ M) with and without addition of $Cu(ClO_4)_2$ ($1.2x10^{-4}$ M) in acetonitrile, λ_{ex} = 340 nm. Addition of metal ion results in the enhancement of excimer band at 470 nm. (b) Fluorescence spectra of **3b** ($1.8x10^{-5}$ M) alone and upon the addition of $AgClO_4$ ($2x10^{-4}$ M) in acetonitrile, λ_{ex} = 290 nm. The fluorescence intensity increases upon addition of $AgClO_4$, indicating the "turn-on" behaviour.

Trp-based compound **3b** was designed with the notion that the indole moiety of tryptophan could bind metal ion by cation-π interactions. Among the various metal ions tested (Na^{+}, K^{+}, Cs^{+}, Ag^{+}, Mg^{2+}, Ba^{2+}, Cd^{2+}, Zn^{2+}, Pb^{2+}, Mn^{2+}, Cu^{2+}, Hg^{2+}, Sn^{2+}, and Fe^{3+}) for binding studies with **3b**, a high selectivity was observed for Ag^{+} (see ESI†, Fig. S1). The absorbance at 285 nm of **3b** decreased upon the addition of Ag^{+} with the concomitant formation of a new band at 314 nm with two isobestic points at 253 and 293 nm. The two isobestic points signified the presence of two species in equilibrium.[12] The appearance of new absorption band at 314 nm is a result of the interaction of indole ring of Trp with Ag^{+} resulting in a strong complex (see ESI†, Fig. S1).[13]

The fluorescence intensity of **3b** increased upon the addition of Ag^{+} (Fig. 1b). The binding studies revealed that **3b** is selective towards Ag^{+} and Job's plot showed a 1:2 stoichiometry between **3b** and Ag^{+} (see ESI†, Figs. S2 and S4). The mass spectra displayed a peak at m/z 691.0371 (see ESI†, Fig. S3) corresponding to **3b** + $2Ag^{+}$ further support the 1:2 complex formation. The binding constant of $1.2x10^{8}$ M^{-2} was obtained by using Benesi-Hildebrand method (see ESI†, Fig. S8) with a detection limit of 8 μM.[11] Competitive binding experiments revealed that **3b** can detect Ag^{+} even in the presence of other cations (see ESI†, Fig. S7). The time resolved fluorescence studies showed that decay time for **3b** (τ= 1.01) is the same as that of **3b** + Ag^{+}, indicating the formation of a complex between **3b** and Ag^{+} (see ESI†, Fig. S6 and Table S2).[10]

Thermodynamics of binding was studied (Fig. 2) by isothermal calorimetry (ITC).[14] **3a** was titrated with Cu^{2+} and the ITC data suggest the formation of 2:1 host-guest complex (2 . **3a**:Cu^{2+}). Similarly, ITC titration of **3b** with Ag^{+} indicated a 1:2 host-guest (**3b**:$2Ag^{+}$) complex. The affinity of the molecules **3a**/**3b** towards Cu^{2+}/Ag^{+} was enthalpy favored (see ESI†, Table S3). The negative free energy term ΔG = -30.18 KJ/mol for the **3a**-Cu^{2+} indicates a thermodynamically favored process. The binding of **3b** with Ag^{+} is also thermodynamically favored as indicated by free energy terms, ΔG_1 = -29.10 KJ/mol and ΔG_2= -47.32 KJ/mol. The binding constants obtained for **3a**-Cu^{2+} and **3b**-Ag^{+} by UV-Visible, fluorescence and ITC are comparable.

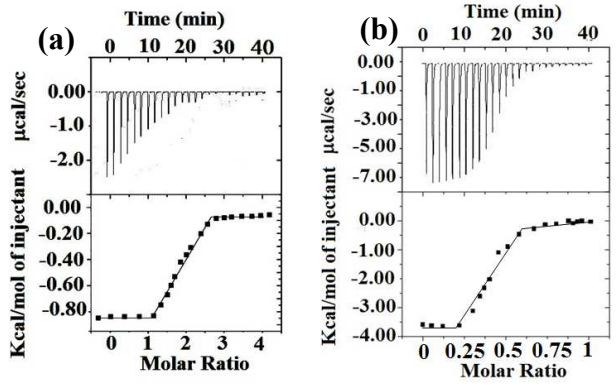

Fig 2. ITC titration data of (a) **3a** [200 μM] with Cu^{2+} (n = 2.09, K_a = $1.95x10^{5}$ M^{-1}) (b) **3b** [150 μM] with Ag^{+} (n = 0.48, K_{a1} = $1.26x10^{5}$ M^{-1} and K_{a2} = $1.97x10^{8}$ M^{-1}). The titrations were performed at 25 °C in acetonitrile. Upper graphs represent experimental data and the bottom panels show the binding isotherms created by plotting the integrated heats from each injection, against the molar ratio of the compounds. Each titration experiment was composed of 19-21 successive injections of 5 μL of metal ions.

Binding interactions of **3a** and **3b** with Cu^{2+} and Ag^{+} were also confirmed by electron microscopy (Fig. 3). The scanning electron microscopic (SEM) analysis of **3a** showed fibrillar morphology, which changes to thick stick-like bars with a length of 824 nm (average of 50 bars) and width of 250 nm (average of 50 bars) as a result of binding with Cu^{2+}. On the other hand, SEM of **3b** showed spherical vesicles, comprised predominantly of two sizes; small vesicles having an average diameter of 458 nm (average of 20 vesicles) and bigger vesicles with an average diameter of 1.41 μm (average of 20 vesicles).

The remarkable ability of **3b** to form vesicular self-assembly is attributed to the presence of indole ring.[15] The presence of indole moiety can acts as a potent H-bond donor and facilitates π-π interactions leading to self-assembled structure. The metal ion binding perturbs the assembly and hence spherical vesicles changes to flower petal like morphology upon binding with Ag^{+} ion (Fig. 3). The completely altered morphologies of **3a** and **3b** with the addition of metal ions further support the interactions of the metal ions with the molecules. Atomic force microscopy (AFM) images also support similar observation (see ESI†, Fig. S9). Interestingly, the self-assembly to bar-shape and petal-like shapes in **3a**/Cu^{2+} and **3b**/Ag^{+} complexes indicate the presence of specific supramolecular interaction in the complexes.

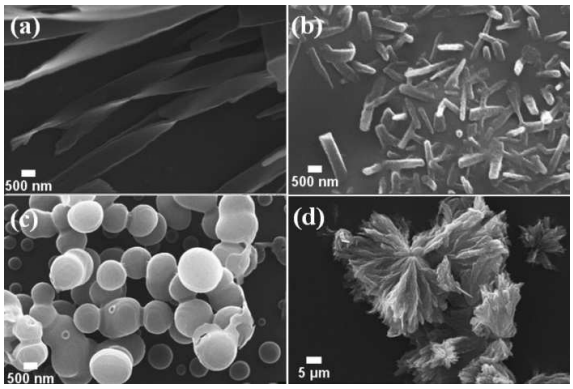

Fig 3. SEM images of (a) **3a** (b) **3a** + Cu^{2+} (c) **3b** (d) **3b** + Ag^{+} in CH_3CN..

The binding modes of **3a** with Cu^{2+} and **3b** with Ag^{+} was investigated by UB3LYP/6-31G(d) level of density functional theory (DFT) and B3LYP/Gen1 level of DFT, respectively where Gen1 corresponds to 6-31G(d) basis set for H, C, N, O and S atoms and LanL2DZ basis set with 'f' polarization function for Ag atom.[16] The calculations are done using the Guassian 09 suite of programs.[17] Several possible 2:1 complexation modes of Cu^{2+} and 1:2 complexation modes of Ag^{+} were studied (see ESI†, Figs. S10-S12). The most stable complex for **3a** with Cu^{2+} (**3a**-Cu^{2+}-**3a**) and **3b** with Ag^{+} (Ag^{+}-**3b**-Ag^{+}) are shown in Fig. 4.

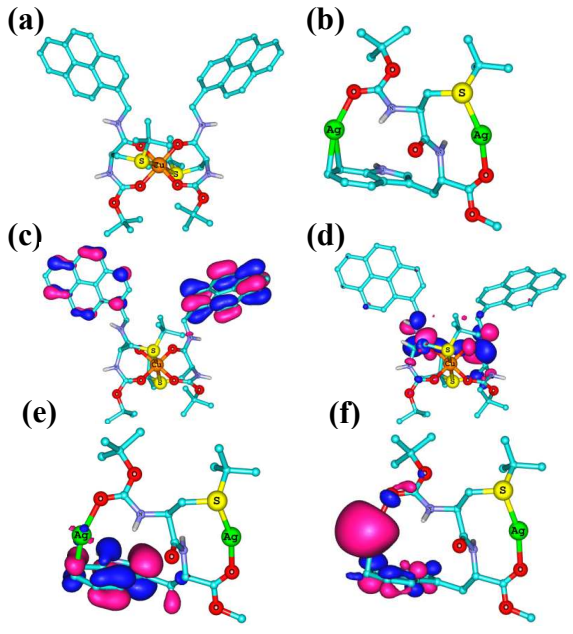

Fig 4. B3LYP/6-31G(d) optimized structure of (a) **3a**-Cu^{2+}-**3a** and (b) Ag^{+}-**3b**-Ag^{+}. (c) HOMO of **3a**-Cu^{2+}-**3a**, (d) LUMO of **3a**-Cu^{2+}-**3a**. (e) HOMO of Ag^{+}-**3b**-Ag^{+} and (f) LUMO of Ag^{+}-**3b**- Ag^{+}. Many hydrogen atoms are omitted for clarity.

The **3a**-Cu^{2+}-**3a** shows an octahedral geometry (Fig. 4a), wherein Cu^{2+} displays a coordination to four carbonyl oxygens of amides in the equatorial positions with an average -O-Cu^{2+}- distance of 1.96 Å and also coordination to two sulfur atoms in the apical positions with average –S-Cu^{2+}- distance of 2.86 Å. The pyrene rings were oriented towards the same side, suggesting the possibility of excimer formation. This is as expected from experimental results from fluorescence studies which indicated the formation of excimer upon Cu^{2+} binding (Fig. 1a). The HOMO of **3a**-Cu^{2+}-**3a** was located on the pyrene rings, while the LUMO was centered on the amide bonds (Figs. 4c and 4d).

The Ag^{+}-**3b**-Ag^{+} structure shown in Figure 4b can be considered as a bicyclic metallomacrocycle (see ESI†, Fig. S12 for seven other binding modes and Table S4). One of the Ag^{+} ions is coordinated by one –S– atom and one amide carbonyl, while the second Ag^{+} ion is coordinated by indole ring of tryptophan residue (Fig. 4b) and another amide carbonyl. The –S-Ag^{+}- and –C-Ag^{+}- distances are 2.48 Å and 2.50 Å respectively, while the average –CO-Ag^{+} distance is 2.21 Å. The HOMO of Ag^{+}-**3b**-Ag^{+} is a π-orbital of indole moiety while the LUMO is centered on one of the Ag atoms (Figs. 4e and 4f).

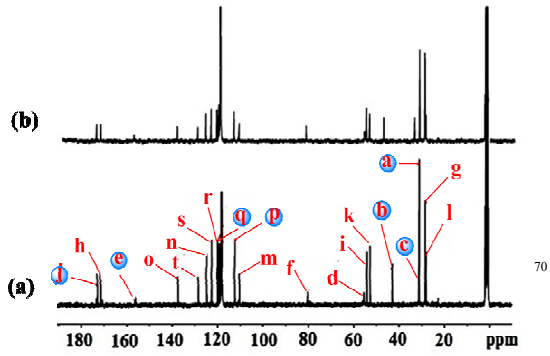

Fig 5. ^{13}C NMR spectra (75 MHz) of (a) **3b** (b) **3b** + Ag^{+} ion in CD_3CN. The blue coloured carbon atoms are involved in Ag^{+} binding.

The binding mode of **3b** with Ag^{+} was supported by ^{1}H NMR as well as by ^{13}C NMR titrations (see ESI†, Figs. S13 and 5).[18] Addition of 0.1 equiv Ag^{+} resulted in an initial shift of –S-CH_2- protons, further addition 0.5 equiv Ag^{+} resulted in splitting of the –S-CH_2- signal. The tryptophan aromatic protons (Hg+Hk+Hj) broadened and shifted down field (see ESI†, Fig. S13). Similarly, the ^{13}C NMR spectra recorded in CD_3CN showed down field shift for the aromatic carbon atoms as well as for the –S-CH_2 carbon atoms. The prominent deshielding effect was observed for the ester (j) as well as for the Boc-carbonyls (e) 0.58 and 0.55 ppm respectively (see ESI†, Table S5). The–S-CH_2- carbon atom (c) deshielded by 0.17 ppm, suggesting the involvement of –S– atom in the binding. The aromatic carbon atoms 'p' and 'q' of the indole ring are deshielded by 0.47 and 0.21 ppm respectively (see ESI†, Table S5 for chemical shifts of carbon atoms), indicating the involvement of these carbons in binding Ag^{+} as was supported by the DFT calculations. Theoretically computed NMR results using the GIAO method[19] also matched very well with the experimental NMR values (see ESI†, Table S5). Thus both the NMR data and the DFT calculations indicate an η^2- type coordination of Ag^{+} with aromatic ring of Trp.[13]

In conclusion, we have designed and synthesized cysteine based fluorescent "turn-on" sensors **3a** and **3b** for Cu^{2+} and Ag^{+} respectively. The design and experimental studies illustrated here highlight that cysteine is a potential amino acid for the design of novel metal ion sensors. Transformation of cysteine to systems with specific metal ion harboring capability is noteworthy. The

results presented here will be useful for the design of novel metal-binding peptide systems. Such peptide systems may find a variety of biomedical applications.

We thank the Department of Science and Technology (DST and DST-FIST) for the financial support. PPPK thanks University Grants Commission (UGC), New Delhi for the fellowship.

Notes and references

1 L. Fabbrizzi, A. Poggi, *Chem. Soc. Rev*., 1995, **24**, 197-202; B.Valeur,I. Leray, *Coord. Chem. Rev*., 2000, **205**, 3-40; (c) L. Prodi, F. Bolletta, M. Montalti, N. Zaccheroni, *Coord. Chem. Rev*., 2000, **205**, 59-83; (d) A. P. de Silva, D. B. Fox, A. J. Huxley, Moody, *Coord. Chem. Rev*., 2000, **205**, 41-57.

2 B. Schazmann, N. Alhashimy, D. Diamond, *J. Am. Chem. Soc*., 2006, **128**, 8607-8614; J. B. Wang, F. X. Qian, J. N. Cui, *J. Org. Chem*. 2006, **71**, 4308-4311; Z. Xu, Y. Xiao, X. Qian, J. Cui, D. Cui, *Org. Lett*., 2005, *7*, 889-892; H. Yuasa, N. Miyagawa, T. Izumi, M. Nakatami, M. Izumi, H. Hashimoto, *Org. Lett*., 2004, **6**, 1489-1492; Z. C. Wen, R.Yang, H. He, Y. B. Jiang, *Chem. Commun*., 2006, 106-108; S. K. Kim, S. H. Lee, J. Y. Lee, R. A. Bartsch, J. S. Kim, *J. Am. Chem. Soc*., 2004, **126**, 16499-16506.

3 T. M. Desilva, G. Veglia, F. Porcelli, A. Prantner, S. J. Opella, *Biopolymers*, 2002, **64**, 189-197; G. Veglia, F. Porcelli, T. Desilva, A. Prantner, S. J. Opella, *J. Am. Chem. Soc*., 2000, **122**, 2389-2390.

4 A. Klung, *Annu. Rev. Biochem*., 2010, **79**, 213-231; A. Klung, *Q. Rev. Biophys*., 2010, **43**, 1-21; D. Jantz, B. T. Amann, G. J. Jr. Gatto, J. M. Berg, *Chem. Rev*., 2004, **104**, 789-799; H. Laity, B. M. Lee, P. E. Wright, *Curr. Opin. Struct. Biol*., 2001, **11**, 39-46.

5 Y. Xue, A. V. Davis, G. Balakrishnan, J. P. Stasser, B. M. Staehlin, P. Focia, T. G. Spiro, J. E. Penner-Hahn, T. V. O'Halloran, *Nat. Chem. Biol*., 2008, **4**, 107-109; K. J. Franz, *Nat. Chem. Biol*., 2008, **4**, 85-86; I. R. Loftin, Ninian, S. Franke, N. J. Blackburn, M. M.Mcevoy, *Protein Sci*., 2007, **16**, 2287-2293.

6 R. M. F. Batista, R. C. M. Ferreira, M. M. M. Raposo, S. P. G. Costa, *Tetrahedron*., 2012, **68**, 7322-7330; L. N. Neupane, J. Y. Park, J. H. Park, K. H. Lee, *Org. Lett*., 2012, **15**, 254-257; M. H. Yang, P. Thirupathi, K. H. Lee, *Org. Lett*., 2011, **13**, 5028-5031.

7 A. P. de Silva, H. Q. N. Gunaratne, T. Gunnlaugsson, A. J. M. Huxley, C. P. McCoy, J. T. Rademacher, T. E. Rice, *Chem. Rev*., 1997, **97**, 1515-1566; F. M. Winnik. *Chem. Rev*., 1993, **93**, 587-614.

8 D. A. Dougherty, *Acc. Chem. Res*., 2013, **46**, 885-893; D. K. Chakravorty, B. Wang, M. N. Ucisik, M. K. Jr. Merz, *J. Am. Chem. Soc*., 2011, **133**, 19330-19333; D. A. Dougherty, *Science*, 1996, **271**, 163-168.

9 L. Fabbrizzi, M. Licchelli, P. Pallavicini, A. Perotti, A. Taglietti, D. Sacchi, *Chem. Eur. J*., 1996, **2**, 75-82; D. J. S. Birch, K. Suhling, A. S. Holmes, T. Salthammer, R. E. Imhof, *Pure Appl. Chem*., 1993, **65**, 1687-1692.

10 G. Petroselli, M. L. Dantola, F. M. Cabrerizo, C. Lorente, A. M. Braun, E. Oliveros, A. H. Thomas, *J. Phys. Chem*., A 2009, **113**, 1794-1799; C. B. Murphy, Y. Zhang, T. Troxler, V. Ferry, J. J. Martin, W. E. Jr. Jones, *J. Phys. Chem*., B 2004, **108**, 1537-1543.

11 L. Ma, H. Li, Y. Wu, *Sensors and Actuators*, B 2009, **143**, 25-29; H. A. Benesi, J. H. Hildebrand, *J. Am. Chem. Soc*., 1949, **71**, 2703-2707.

12 G. Scheibe, *Angew. Chem. Int. Ed*., 1937, **50**, 212-219; M. D. Cohen, E. Fischer, *J. Chem. Soc*., 1962, **3**, 3044-3052.

13 I. R. Loftin. N. J. Blackburn. M. M. McEvoy. *J. Biol. Inorg. Chem*., 2009, **14**, 905-912; O. Kuhl, W. Hinrichs, *Chem Bio Chem*., 2008, **9**, 1697-1699.

14 V. D. Jadhav, F. P. Schmidtchen, *Org. Lett*., 2005, **7**, 3311-3314; A. Cooper, *Curr. Opin. Chem. Biol*., 1999, **3**, 557-563.

15 E. Abel, S. L. De Wall, W. B. Edwards, S. Lalitha, D. F. Covey, G. W. Gokel, *J. Org. Chem*., 2000, **65**, 5901-5909; E. Abel, M. F. Fedders, G. W. Gokel, *J. Am. Chem. Soc*., 1995, **117**, 1265-1270.

16 A. D. Becke, *J. Chem. Phys*., 1993, **98**, 5648-5652; A. W. Ehlers, M. Böhme, S. Dapprich, A. Gobbi, A. Höllwarth, V. Jonas, K. F. Köhler, R. Stegmann, A. Veldkamp, G. Frenking, *Chem. Phys. Lett*., 1993, **208**, 111-114.

17 M. J. Frisch, et al. Gaussian 09, Revision C.01, 2010.

18 Y. Li, C.M. Yang, *J. Am. Chem. Soc*., 2005, **127**, 3527-3530; H. Sun, E. Oldfield, *J. Am. Chem. Soc*., 2004, **126**, 4726-4734.

19 K. Wolinski, J. F. Hilton, P. Pulay, *J. Am. Chem. Soc*., 1990, **112**, 8251-8260.

Cysteine-based fluorescence "turn-on" sensors for Cu^{2+} and Ag^{+}

V. Haridas *, P. P. Praveen Kumar and Cherumuttathu H. Suresh

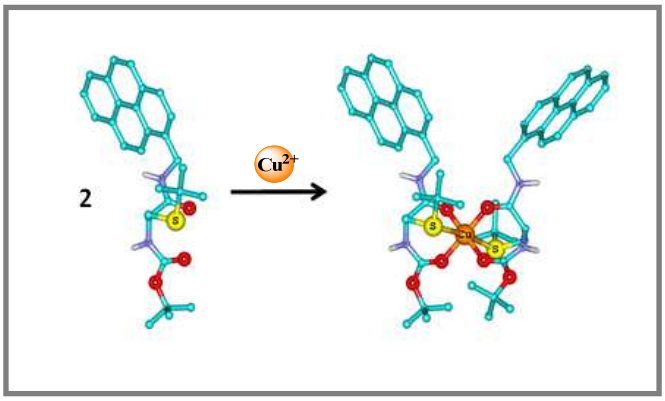

Amino acid cysteine was transformed to fluorescent TURN ON sensors for Cu^{+2} and Ag^{+}. The metal ion binding was studied in detail by spectroscopic, microscopic, calorimetric and computational methods.